

## Cu<sub>2</sub>O/ZnO NANOCOMPOSITE AND GRAPHENE OXIDE WITH PHOTOCATALYSIS FOR TEXTILE DYES/DYE REDUCTION

FRIKSON JONY PURBA<sup>1</sup>, KERISTA TARIGAN<sup>2</sup>, ZURIAH SITORUS<sup>3</sup>, NURDIN SIREGAR<sup>4</sup>, ERNA FRIDA<sup>5</sup>, NURDIN BUKIT<sup>6</sup> and DEDI HOLDEN SIMBOLON<sup>7</sup>

<sup>1, 2, 3, 5</sup>University of Sumatera Utara, Medan, Indonesia

<sup>4, 6</sup>State University of Medan, Indonesia

<sup>7</sup>University of Quality Medan, Indonesia

### Abstract

Nanocomposite photocatalyst materials have been made from a mixture of raw materials for Cu<sub>2</sub>O nanoparticles, ZnO nanoparticles and graphene oxide (GO) through coprecipitation and hydrothermal methods with variations in the composition of Cu<sub>2</sub>O/ZnO nanocomposites before adding GO dopant, namely the ratio Cu<sub>2</sub>O:ZnO 1:1, 1:2 and 2:1 and Cu<sub>2</sub>O/ZnO/GO nanocomposites after added GO with composition variations of 1%, 3%, 5% and 10%. Sampling was carried out in two steps. The first step was the synthesis of Cu<sub>2</sub>O and ZnO nanoparticles using Cu(NO<sub>3</sub>)<sub>2</sub>·3H<sub>2</sub>O and Zn(NO<sub>3</sub>)<sub>2</sub>·6H<sub>2</sub>O precursors based on the coprecipitation method and graphene oxide derived from graphite oxide (pencil rods) using a modified hummer method. The second step is mixing Cu<sub>2</sub>O, ZnO, and GO nanoparticles using the hydrothermal method to form Cu<sub>2</sub>O/ZnO/GO nanocomposites which are then characterized including: physical properties with FESEM-EDS (surface morphology and elemental content), BET (specific surface area, pore volume and size), and XRD (crystal structure and size of crystalline diameter), chemical properties with FTIR (functional groups), optical properties with Uv-Vis (absorbance value and energy gap), and photocatalytic performance properties with photoluminescence (photocatalytic activity). The characterization results showed that the most optimum composition was Cu<sub>2</sub>O/ZnO nanocomposite with a ratio of 1:2 and the addition of 5% GO resulted in a specific surface area of 35.115 m<sup>2</sup>/g with a pore radius of 1.9073 nm, a pore volume of 0.094 cm<sup>3</sup>/gr and a crystalline diameter of 0.27368 nm has an absorbance value of 0.115, an energy gap of 1.85 eV and a degradation efficiency of 85.9% methylene blue under UV light from a halogen lamp for 120 minutes. The results of photocatalytic materials based on Cu<sub>2</sub>O/ZnO/GO nanocomposite can be applied to degrade methylene blue textile dye waste.

Keywords: Cu<sub>2</sub>O/ZnO/GO Nanocomposites, Graphene Oxide, Methylene Blue, Photocatalytic Method, Textile Dyes Waste Degradation

### INTRODUCTION

Along with the development activities of the textile industry at this time, it does not directly have an impact on the decline in environmental quality, especially the quality of polluted air in the process of industrial production activities. In general, most industries use a lot of organic dyes in the coloring process of their production. This is very dangerous if the dye waste is directly discharged into the river without any waste treatment first, because the waste will not be environmentally friendly and will be difficult to degrade naturally. Another problem is the increasing demand for clean water

due to the consumption of clean water, resulting in a large amount of wastewater. Therefore, wastewater treatment has become one of the biggest challenges of this century (H. Yan et al 2021).

Waste produced by textile factories usually contains high levels of azo dyes consisting of benzene bonds (M. Zhang et al 2020). Considering the stability of the dyes and their potential toxicity in water, various purification methods such as adsorption, coagulation and advanced oxidation processes have been previously carried out to reduce the effluent containing large amounts of various dyes (B. Chandu et al 2020). The advanced oxidation process is a promising technology because it is able to efficiently produce chemical structure transformations for various contaminated waters, through oxidation reactions such as hydroxyl radicals (Y. Sheng et al 2019).

In addition, a common method for removing organic dyes is adsorption treatment using an adsorbent (X. Huang et al 2019). To date, various types of adsorbents have been developed, such as inorganic compounds, polymers, and carbon-based materials and these adsorbents can be made into fibers, membranes and foams (R. T. Ginting, et al 2018). Adsorption capacity (mg/g) is a parameter that is widely used to test the adsorption ability of adsorbents against certain organic dyes. In general, higher adsorption capacity means better adsorption ability. Different adsorption mechanisms, such as electrostatic interactions, ion exchange,  $-\pi$  interactions, and hydrogen bond formation, have been proposed based on the interactions between organic dyes and adsorbents (S. Kaur et al 2017). However, all these adsorbents face the same problem. The adsorbed organic dye must be removed from the adsorbent using other chemical reagents (desorption process), such as strong acid or strong alkali, so that the adsorbent can be reused. The desorption treatment not only leads to an increase in the cost of wastewater treatment, but also faces new problems because the adsorption efficiency decreases with the destruction of the adsorbent structure during the desorption treatment (J. Jiang et al 2019).

From various advanced oxidation processes such as ozonation process, Fenton and adsorption methods, heterogeneous photocatalysis process (E. Jang et al 2019) offers a more economical technology, fast oxidative reaction, without harmful substances and environmentally friendly. Degradation method of waste treatment by photocatalytic process can reduce organic dye levels efficiently. Of the various types of photocatalysis, semiconductor materials such as titania ( $\text{TiO}_2$ ), zinc oxide and cuprum oxide ( $\text{Cu}_2\text{O}$ ) have attracted the researchers' attention more (B. T. Gadisa et al 2020). Among these semiconductor materials, the photocatalytic degradation ability of  $\text{Cu}_2\text{O}$  and its application has become one of the main research subjects because  $\text{Cu}_2\text{O}$  is an environmentally friendly p-type semiconductor material with a small bandgap energy ( $E_g$ ) of about 2.0-2.2 eV indicating that photocatalytic degradation activity of  $\text{Cu}_2\text{O}$  can be affected with the help of sunlight (Kumar and Rao 2015). However, similar to other semiconductor materials, pure  $\text{Cu}_2\text{O}$  still exhibits low photocatalytic degradation of

organic dyes in its application, due to the rapid recombination of electron-hole pairs after light absorption. Therefore, the main key that ensures the achievement of efficient photocatalytic degradation of Cu<sub>2</sub>O is to realize the electron and hole separation produced by light absorption (T. Zhou et al 2018).

Incorporating other materials as electron acceptors is an alternative way to increase the efficiency of photocatalytic degradation by Cu<sub>2</sub>O. Various materials have been used to make photocatalysts based on Cu<sub>2</sub>O composites, such as n-type semiconductors (ZnO and TiO<sub>2</sub>), conductive polymer polyaniline (PANI), graphene and graphene oxide (GO) (Dasineh et al 2019). Of various materials, ZnO and GO are more promising as composites for Cu<sub>2</sub>O because ZnO has an energy band gap of 3.2 eV, an excitation binding energy of 60 MeV and efficient electron and hole separation (Chou et al 2017). In addition, GO can be assumed as a semiconductor material (sp<sup>2</sup> hybridization structure) which has chromophoric properties so that it can absorb free electrons quickly with an electron mobility of 200,000 cm<sup>2</sup>/Vs and a specific surface area of 2630 m<sup>2</sup>/g. produced by Cu<sub>2</sub>O can easily be transferred to GO so as to avoid recombination of electron and hole pairs (M. Asgharian 2019). Second, the GO surface consists of chemical bonds containing oxygen and is suitable for adsorption of organic dyes thereby increasing the efficiency of photocatalytic degradation of the composite.

Therefore, from the advantages of each material, ZnO and GO are very promising to increase the efficiency of photocatalytic degradation of Cu<sub>2</sub>O/ZnO/GO nanocomposites against methylene blue organic dyes.

## 2 METHODOLOGY

### 2.1 Subjects

For the preparation of Cu<sub>2</sub>O and ZnO nanoparticles, graphene oxide (GO) and Cu<sub>2</sub>O/ZnO and Cu<sub>2</sub>O/ZnO/GO nanocomposites as photocatalyst materials for methylene blue. Meanwhile, the characterization of nanocomposite photocatalyst includes physical, chemical, optical and photocatalytic activity. A total of 0.2 g of PVP (Polyvinylpyrrolidone) was added to a beaker containing 190 mL EG, and then mixed and stirred at 40 °C to ensure complete mixing of PVP and EG.

### 2.2 Research Design and Instruments

A total of 3 mmol Zn (NO<sub>3</sub>)<sub>2</sub>·6H<sub>2</sub>O was dissolved in 50 mL distilled water and 6mmol C<sub>6</sub>H<sub>5</sub>Na<sub>3</sub>O<sub>7</sub>·2H<sub>2</sub>O was slowly added to the solution while stirring until the solution became clear. After that, 10 mL of 0.1 M NaOH solution was added by drop into the above solution and stirred for 2 hours at room temperature.

### 2.3 Data Collection Procedures

The graphene oxide synthesis process was carried out using a modified Hummer method. A total of 2 grams of graphite powder was dissolved in 98 mL of 98% H<sub>2</sub>SO<sub>4</sub>, and then 4 grams of NaNO<sub>3</sub> were added during the stirring process for 1 hour. The addition of 8 grams of KMnO<sub>4</sub> was carried out gradually into the mixture after stirring lasted 2 hours. For 4 hours the temperature was maintained at a temperature range of 20°C to 35°C. The mixture is stirred slowly until it turns a greenish black color. The stirring process was continued for 20 hours at 35°C. First, to find out which nanocomposites are suitable for Cu<sub>2</sub>O and ZnO, various ratios between Cu<sub>2</sub>O and ZnO were tested, namely 1:1, 1:2, and 2:1 which were then tested by FESEM-EDS (surface morphology and elemental content), BET (surface area). Specific, pore volume and pore size), and XRD (crystal structure and crystalline diameter), chemical properties namely FTIR (functional group), optical properties namely Uv-Vis (absorbance value and energy gap), and photocatalytic performance properties namely Photoluminescence (photocatalytic degradation activity). After obtaining the optimum ratio, Cu<sub>2</sub>O/ZnO/GO will be composited with graphene oxide using hydrothermal with different composition variations of 4 different parameters and respectively 1%, 3%, 5% and 10%. Furthermore, characterization of physical properties, chemical properties, optical properties and photocatalytic degradation activity on the efficiency of reducing the concentration of the best methylene blue dye under UV irradiation from a halogen lamp.

## 4 RESULT ANALYSIS

In Cu<sub>2</sub>O/ZnO/GO Nanocomposite Photocatalyst Cu<sub>2</sub>O/ZnO/GO Nanocomposite as methylene blue photocatalyst in textile waste produced by a series of synthesis processes with co-precipitation and hydrothermal methods. Cu<sub>2</sub>O/ZnO nanoparticles were carried out using Cu(NO<sub>3</sub>)<sub>2</sub>·3H<sub>2</sub>O and Zn(NO<sub>3</sub>)<sub>2</sub>·6H<sub>2</sub>O precursors which were reactive to easily produce Cu<sub>2</sub>O and ZnO when in contact with water with various compositions of Cu<sub>2</sub>O/ZnO nanocomposite before being added with graphene oxide (GO) dopants. I.e. with a ratio of 1:1, 2:1 and 1:2 and after being composited with GO with the addition of GO 1%, 3%, 5% and 10%. Then the Cu<sub>2</sub>O/ZnO/GO nanocomposite was characterized to see how the interactions between the internal materials formed on physical properties: surface morphology, crystal structure, and porosity size, chemical properties: functional groups, optical properties: photon absorption based on energy gap and performance properties: methylene degradation. blue-based photocatalytic activity (Hung et al 2020). In this case, the parameters that affect the properties of the material include the effect of the composition of GO dopants to provide an overview of the interactions in forming a bond between a mixture of one material and another. It also looks at the possible by-products of the products contained in the nanocomposite.

## 5 DISCUSSION

Following are the results of the X-ray diffraction pattern of Cu<sub>2</sub>O/ZnO nanocomposite before being inserted by GO with variations in the Cu<sub>2</sub>O:ZnO concentration ratio of 1:1, 1:2 and 2:1, respectively, as shown in Figure 1:

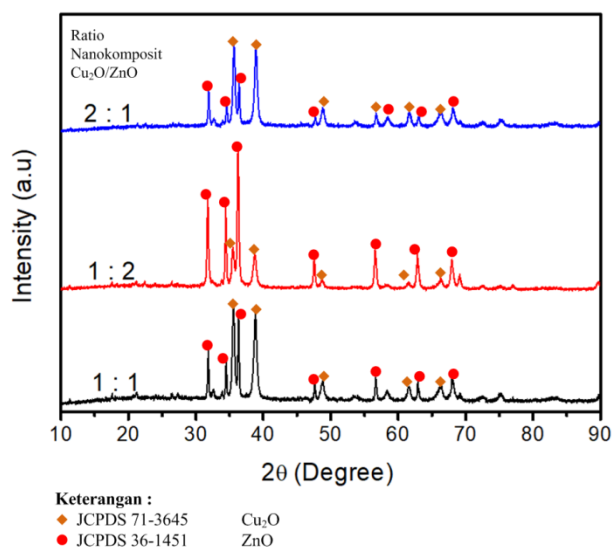


Fig. 1. XRD Diffraction Pattern Spectrum of Cu<sub>2</sub>O/ZnO Nanocomposite Photocatalysts with Composition Ratios of 2:1, 1:2 and 1:1

Furthermore, it can be seen in Figure 1 which shows the difference in peaks from XRD test results from Cu<sub>2</sub>O/ZnO nanocomposite materials with the addition of 1%, 3%, 5%, and 10% GO, almost no significant difference. It can be seen in the figure that there are ZnO peaks located in almost all the peaks of the nanocomposite diffraction pattern. This means that the presence of ZnO in the photocatalyst Cu<sub>2</sub>O/ZnO/GO nanocomposite dominates because ZnO is present at the highest peak of the XRD diffraction pattern. Then there was a change in the value of the diffraction pattern of the highest peaks indicating that Cu<sub>2</sub>O and GO had been successfully combined with ZnO to form Cu<sub>2</sub>O/ZnO/GO nanocomposites which resulted in changes in the intensity peak values (S. Baizaee et al 2018). However, the pattern of the diffraction peaks for graphene oxide (GO) is not clear due to the change in the structure to amorphous which causes the crystallinity level to decrease so that the effect of the appearance of graphite oxide peaks during the reduction process so that it becomes an impurity in the graphene oxide

material. In addition, GO has crossed the solubility limit of Cu<sub>2</sub>O/ZnO nanocomposite so that it is segregated due to the very low concentration of GO. The following are the peaks of the material diffraction pattern in practice using the MATCH Vers.1.1.1 software analysis, namely:

TABLE 1  
 THE HIGHEST PEAK RESULT OF THE DIFFRACTION PATTERN OF Cu<sub>2</sub>O/ZnO/GO  
 PHOTOCATALYTIC NANOCOMPOSITE SAMPLES

Sampel	Peak to-	2θ (deg)	d <sub>spasi</sub> (Å)	hkl
Cu <sub>2</sub> O/ZnO/GO 1%	1	36,23	2,4774	[1 0 1]
	2	31,75	2,8160	[1 0 0]
	3	34,41	2,6042	[0 0 2]
Cu <sub>2</sub> O/ZnO/GO 3%	1	36,24	2,4788	[1 0 1]
	2	31,76	2,8175	[1 0 0]
	3	34,42	2,6056	[0 0 2]
Cu <sub>2</sub> O/ZnO/GO 5%	1	36,23	2,4774	[1 0 1]
	2	31,73	2,8178	[1 0 0]
	3	34,39	2,6057	[0 0 2]
Cu <sub>2</sub> O/ZnO/GO 10%	1	36,26	2,4754	[1 0 1]
	2	31,76	2,8152	[1 0 0]
	3	34,44	2,6020	[0 0 2]

Characterization of Field Emission Scanning Electron Microscope (FE-SEM)-EDS analysis. In the FE-SEM test, photocatalytic samples were carried out on Cu<sub>2</sub>O/ZnO nanocomposites at ratios of 1:1, 1:2, and 2:1, and Cu<sub>2</sub>O/ZnO/GO nanocomposites. With variations in the addition of 1%, 3%, 5% and 10% GO which serves to determine the shape of the surface morphology of the nanocomposite which can be shown in Figure 2 with a magnification of 5000 times as follows:

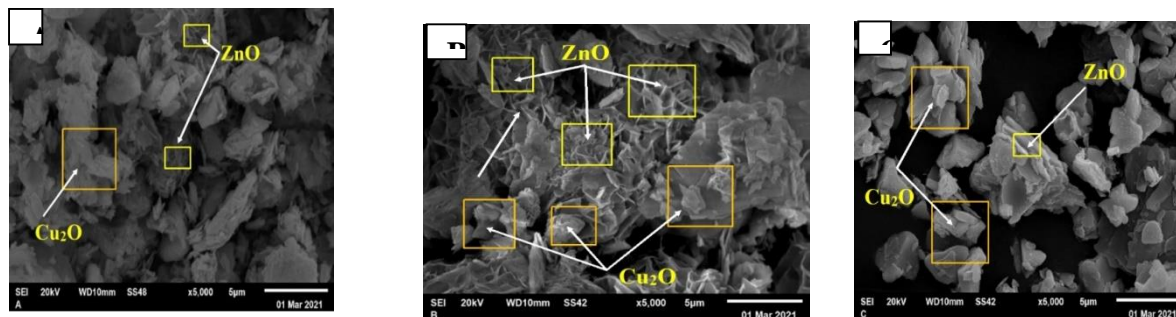


Fig. 2. 5000x SEM Micrograph on Cu<sub>2</sub>O/ZnO Nanocomposite Samples with Composition Ratio; (a) 1:1 (b) 1:2 and (c) 2:1

And GO acts as a barrier to the accumulation of Cu<sub>2</sub>O/ZnO nanocomposites so that a large specific surface area of Cu<sub>2</sub>O/ZnO photocatalysts is produced so that it can increase

photocatalytic activity. Following are the results of FE-SEM morphology of Cu<sub>2</sub>O/ZnO nanoparticles with a 1:2 ratio that have been composited with graphene oxide (GO) with a magnification of 25,000 times, namely:

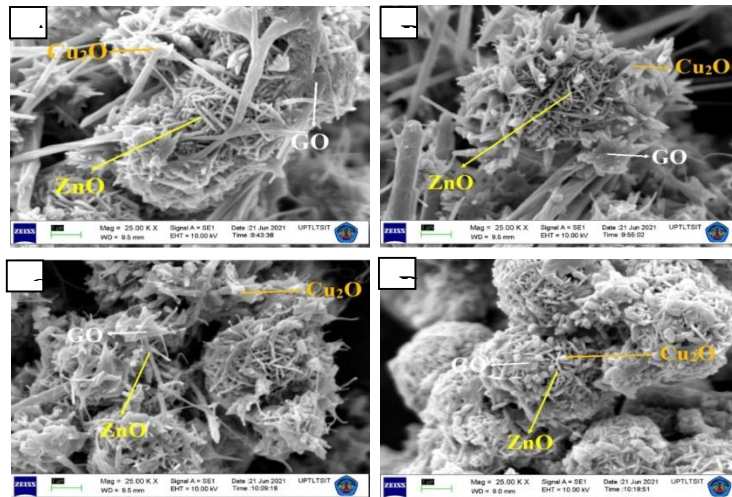


Fig. 3. 25.000x FE-SEM Micrograph on Cu<sub>2</sub>O/ZnO/GO Nanocomposite Photocatalyst Samples with the Addition of Variations in Graphene Oxide (GO) Composition; (a) 1%, (b) 3%, (c) 5%, and (d) 10%

Graphene oxide obtained from the synthesis of graphite material through the modified hummer method has morphology with irregular flakes. After the graphite is oxidized to graphite oxide, the resulting morphology becomes layered sheets so that it looks thick. Then the graphite oxide is reduced to GO so that it looks like thinner but stacked sheets of GO formed by chemical exfoliation of graphite oxide. Then for Cu<sub>2</sub>O nanoparticles still in the form of nanocubes attached to the surface of the ZnO structure and spread (N. Kumaresan et al 2020). Whereas ZnO nanoparticles previously had a morphological structure such as rods (cylindrical rods/tubes) which had irregular lengths, but when ZnO nanoparticles were composited with GO dopant material, the morphological structure of ZnO changed into needle structures with irregular sizes. After that, the average size of the rod-shaped ZnO nanoparticles obtained from the calculation of the Scherrer equation is about 0.27368 nm.

In order to investigate the functional group of various molar ratios of Cu<sub>2</sub>O/ZnO nanocomposites, FTIR analysis was performed. Figure 3 shows the FTIR spectra with sharp peak at 3450 cm<sup>-1</sup> can be ascribed to the stretching vibrations of OH group due to moisture content in nanocomposites samples. Strong peak at 545 cm<sup>-1</sup> which assigned to the Zn-O bond. Sharp peak at 640 cm<sup>-1</sup> corresponds to the stretching vibration band Cu-O mainly originated from Cu<sub>2</sub>O, meanwhile sharp peak at 895 cm<sup>-1</sup> can be associated with vibrational frequencies due to the Cu incorporated into ZnO lattice. In addition, the stronger peak at 1496 cm<sup>-1</sup> can be correlated to the deformation of

carboxylic group (-OH). Accordingly, the sharp peak of carboxylic group of 1:2 samples was observed as compared to 1:1 and 2:1 samples.

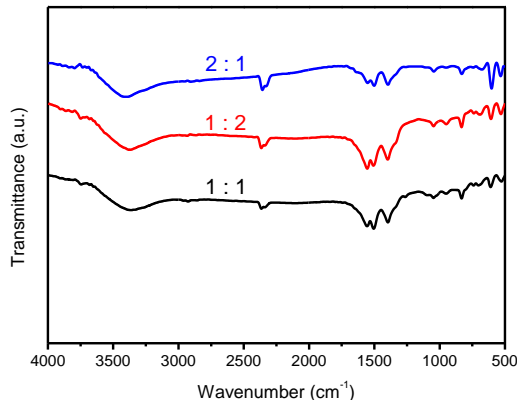


Fig. 4. FTIR spectra of Cu<sub>2</sub>O/ZnO nanocomposites with various molar ratio of Cu(NO<sub>3</sub>)<sub>2</sub> and Zn(CH<sub>3</sub>CO<sub>2</sub>)<sub>2</sub>.

To further elucidate the crystallinity of Cu<sub>2</sub>O/ZnO nanocomposites was investigated. The XRD patterns of nanocomposites were shown in Figure. 3. The XRD peak at 31.73, 34.44 and 36.34 ° can be associated to (100), (002) and (101) planes of ZnO. In addition, the other ZnO peaks was found at 47.72, 56.74, 62.86, 66.26, 68.10 and 69.12 ° related to (102), (110), (103), (200), (112) and (201) planes, respectively. These further confirm the evidence of wurtzite ZnO. Moreover, the other diffraction peak at 32.68, 35.50, 38.84 ° were correspond to the (110), (-111) and (111), respectively which confirm the monoclinic structure of Cu<sub>2</sub>O. This result was similar with previous report on ZnO/CuO decorated with rGO composites. Interestingly, the overall diffraction peaks for 1:2 sample was higher for Cu<sub>2</sub>O and ZnO peaks compared to 1:1 and 2:1 samples as expected from SEM images.

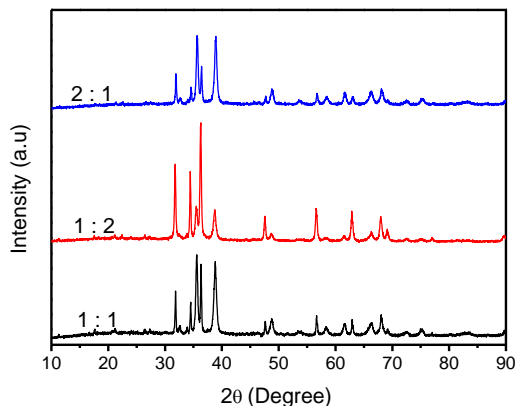


Fig. 5. XRD patterns of Cu<sub>2</sub>O/ZnO nanocomposites with various molar ratio of Cu(NO<sub>3</sub>)<sub>2</sub> and Zn(CH<sub>3</sub>CO<sub>2</sub>)<sub>2</sub> (1:1, 1:2 and 2:1).



Photocatalytic degradation of MB (concentration of 5 ppm) with  $\text{Cu}_2\text{O}/\text{ZnO}$  nanocomposites was investigated under visible light irradiation. Figure 5 a-c shows the UV-Vis absorption spectra of MB at different visible light irradiation time with various molar ratio of  $\text{Cu}_2\text{O}/\text{ZnO}$  nanocomposites (1:1, 1:2 and 2:1) photocatalyst. It can be clearly seen that the MB absorbance decreases with increasing irradiation time, thus MB concentration in the solution is gradually reduced in presence of both photocatalysts. Initially, no considerable degradation can be observed under dark conditions, which suggesting that the MB was degraded due to photocatalytic activity. MB absorbance almost disappears after irradiation for 120 min in the presence of  $\text{Cu}_2\text{O}/\text{ZnO}$  photocatalyst as shown in Figure 9b. The  $C/C_0$  of MB degradation against irradiation time with the addition of  $\text{Cu}_2\text{O}/\text{ZnO}$  photocatalyst was compared and plotted in Figure 5. It was observed that the photodegradation of MB with  $\text{Cu}_2\text{O}/\text{ZnO}$  nanocomposites after 120 min with ratio 1:1, 1:2 and 2:1 reaches  $C/C_0$  35, 4 and 51 %, respectively which correlated to the photocatalytic efficiency of 65, 96 and 49 %. The difference of the MB photodegradation mainly due to the morphology, functional groups, and crystalline properties are the main reason for this different photocatalytic activity. The highest photocatalytic efficiency achieved by molar ratio of 1:2 sample, which is supported by XRD finding with higher crystallinity compared to other sample (Abdolhoseinxadeh and Sheibani 2020). Even though the sample exhibit higher photocatalytic efficiency, however, it is still lower than previously reported  $\text{Cu}_2\text{O}/\text{ZnO}$  with degradation rate of 98 %. This could be due to the fact that this works using simple, low-cost and low output power of halogen light. Besides, facile and low temperature synthesis along with optimum performance under visible light allowed this material to be used on a larger scale.

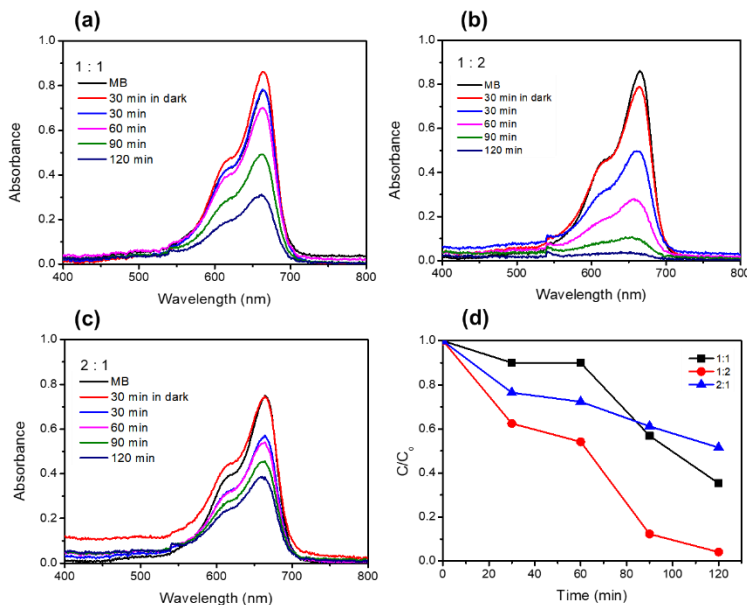


Fig. 6. UV-visible absorbance spectra presented the concentration of MB aqueous

solution in the presence of Cu<sub>2</sub>O/ZnO nanocomposites with molar ratio of (a) 1:1, (b) 1:2 and (c) 2:1; (d) time dependent of photocatalytic degradation from 0 to 120 min under visible light irradiation.

## CONCLUSION

The manufacture of nanocomposite-based photocatalyst materials from the incorporation of Cu<sub>2</sub>O and ZnO nanostructures using the coprecipitation method from the synthesis of Cu(NO<sub>3</sub>)<sub>2</sub>·3H<sub>2</sub>O and Zn(NO<sub>3</sub>)<sub>2</sub>·6H<sub>2</sub>O precursors for degradation applications of methylene blue (MB) in textile dye waste has been carried out. In this study, the Cu<sub>2</sub>O/ZnO nanocomposite which was synthesized hydrothermally produced the optimum composition at the Cu<sub>2</sub>O:ZnO ratio of 1:2 with the characteristics of producing a homogeneous surface morphology and visible hexagonal wurtzite crystal structure in the form of rods and monoclinic in the form of a clear nanocube with a crystalline diameter of 0.27368 nm, specific surface area 23.433 m<sup>2</sup>/gr, average pore radius 0.844 nm and pore volume 0.77 cm<sup>3</sup>/g composed of the main groups -OH, C=C and CH with wave numbers 3367.91 cm<sup>-1</sup>, 1555, 20 cm<sup>-1</sup>, and 1398.37 cm<sup>-1</sup>, absorbance value 0.109, energy gap 1.91 eV and degradation efficiency of 97.9% methylene blue for 120 minutes under UV light from a halogen lamp. It was found that the addition of graphene oxide (GO) dopant material on Cu<sub>2</sub>O/ZnO/GO nanocomposite as the most optimal photocatalyst material was 5% which resulted in a specific surface area of 35,115 m<sup>2</sup>/g with a pore radius of 1.9073 nm and a pore volume of 0.094 cm<sup>3</sup>/gr produces an absorbance of 0.115, an energy gap of 1.85 eV and a degradation efficiency of MB 85.9%.

## REFERENCES

- 1) H. Yan, C. Lai, D. Wang, S. Liu, X. Li, X. Zhou, H. Yi, B. Li, M. Zhang and L. Li, *Journal of Materials Chemistry A* (2021).
- 2) M. Zhang, Z. Zhang, S. Liu, Y. Peng, J. Chen and S. Y. Ki, *Ultrason. Sonochem.* **65**, 105058 (2020).
- 3) B. Chandu, C. M. Kurmarayuni, S. Kurapati and H. B. Bollikolla, *Carbon Letters* **30** (2), 225-233 (2020).
- 4) Y. Sheng, J. Yang, F. Wang, L. Liu, H. Liu, C. Yan and Z. Guo, *Appl. Surf. Sci.* **465**, 154-163 (2019).
- 5) X. Huang, R. Wang, T. Jiao, G. Zou, F. Zhan, J. Yin, L. Zhang, J. Zhou and Q. Peng, *ACS omega* **4** (1), 1897-1906 (2019).
- 6) R. T. Ginting, E.-B. Jeon, J.-M. Kim, W.-Y. Jin and J.-W. Kang, *ACS applied materials & interfaces* **10** (37), 31291-31299 (2018).
- 7) R. T. Ginting, S. Kaur, D.-K. Lim, J.-M. Kim, J. H. Lee, S. H. Lee and J.-W. Kang, *ACS applied materials & interfaces* **9** (41), 36111-36118 (2017).
- 8) J. Jiang, Z. Mu, H. Xing, Q. Wu, X. Yue and Y. Lin, *Appl. Surf. Sci.* **478**, 1037-1045 (2019).
- 9) E. Jang, D. W. Kim, S. H. Hong, Y. M. Park and T. J. Park, *Appl. Surf. Sci.* **487**, 206-210 (2019).
- 10) B. T. Gadisa, S. K. Kassahun, R. Appiah-Ntiamoah and H. Kim, *J. Colloid Interface Sci.* **570**, 251-263 (2020).
- 11) S. G. Kumar and K. K. Rao, *Rsc Advances* **5** (5), 3306-3351 (2015).
- 12) T. Zhou, Z. Zang, J. Wei, J. Zheng, J. Hao, F. Ling, X. Tang, L. Fang and M. Zhou, *Nano Energy* **50**, 118-125 (2018).

- 13) N. Dasineh Khiavi, R. Katal, S. Kholghi Eshkalak, S. Masudy-Panah, S. Ramakrishna and H. Jiangyong, *Nanomaterials* **9** (7), 1011 (2019).
- 14) Y.-C. Pu, H.-Y. Chou, W.-S. Kuo, K.-H. Wei and Y.-J. Hsu, *Applied Catalysis B: Environmental* **204**, 21-32 (2017).
- 15) M. Asgharian, M. Mehdipourghazi, B. Khoshandam and N. Keramati, *Chem. Phys. Lett.* **719**, 1-7 (2019).
- 16) L. T. Dat, N. T. Hung and V. A. Tuan, *Vietnam Journal of Chemistry* **58** (4), 517-525 (2020).
- 17) S. Baizae, M. Arabi and A. Bahador, *Mater. Sci. Semicond. Process.* **82**, 135-142 (2018).
- 18) N. Kumaresan, M. M. A. Sinthiya, K. Ramamurthi, R. R. Babu and K. Sethuraman, *Arabian Journal of Chemistry* **13** (2), 3910-3928 (2020).
- 19) A. Abdolhoseinzadeh and S. Sheibani, *Adv. Powder Technol.* **31** (1), 40-50 (2020).